Sentinel-2 Satellite Imagery based Population Estimation Strategies at FabSpace 2.0 Lab Darmstadt

Md Bayzidul Islam [(1)], Matthias Becker [(1)], Damian Bargiel [(1)], Kazi Rifat Ahmed [(1)], Philipp Duzak [(2)], Nsikan-George Emana [(2)]

(1) Darmstadt University of Technology, Darmstadt, Germany
bislam@psg.tu-darmstadt.de
(2) Goethe University Frankfurt, Frankfurt, Germany

Abstract. This paper elaborates the Sentinel-2 image processing approaches used for the estimation of the population of an area of interest at Image CLEF Remote 2017 lab by the FabSpace 2.0 Darmstadt team. The task is introduced by Image CLEF Lab as a new pilot task in 2017 (Remote) which aims at exploring Copernicus Earth Observation data (i.e. Sentinel-2 satellite imagery) in order to estimate the population of an area of interest [2]. Therefore, the pilot task is focusing on mapping human settlement to estimate population using Sentinel-2 data for humanitarian activities and/or establishing communication infrastructure etc. Human societies and civilizations have been expanding with consequent impact throughout the decades. The expansion of human societies has wider implication in relation to the physical environment and other natural resources. Therefore, it could be a fundamental potential of technological innovation in supporting human activities and sufferings throughout mapping diverse human societies in the world. Although there exist a lot of previous studies used commercial and non-commercial high to moderate resolution satellite imagery for the estimation of the population, this study will investigate the potential of the new Sentinel-2 European satellites. They provide data with 10 m resolution imagery for free, thanks to the Copernicus open data policy for all imagery in five days interval. Thus the use of Sentinel-2 data to develop any new application i.e. population estimation can be cost effective and is reasonably accurate.

Keyword: Sentinel-2, Population Estimation, Classification, Lusaka, Uganda

1 Introduction

The dispersal and distribution of human population through decades has been observed with attendant impacts. As the human society evolves and expands with accompanying changes in the demographic structure; inevitable consequences on the environment is and has been manifesting and will continue to

manifest. These manifestations have wider implications for the society through its interactions with different sectors: markets, the physical environment, urbanization (through urban heat island), ecosystems, food, water and other natural resources. Although emphasis on climate and land use change [16] as well as pollution has often been cited as environmental consequences of growing population density across scales; other challenges like migration with shifts in pressure from one geographic space to another have been documented [15] [30].

However, when viewed from the prism of globalization and an Information and Communication Technology - ICT -driven and ICT-enabled society, human population expansion in all its three dimensions, size, distribution and composition [16] could offer incredible potential for markets and technological innovations. Such potential can only be realized if there are empirically -validated means or methods of mapping human population and demonstrating how these means can support policy reviews and recommendations on the mitigation or promotion of certain developments depending on the objective. It has also been noted that there is a huge potential for markets and innovations in technology arising relevant policy instruments on growing human population [8] [32].

Remote Sensing and Geographic Information System GIS) offer this scientific opportunity in mapping the size and distribution of population at spatio-temporal scale. In the following studies which have addressed the application of remote sensing in mapping of human population dynamics. Remote sensing therefore has the capability of supporting areal interpolation and statistical modelling methods of population studies by Jensen and Cowen 1999 [19], Dobson, Bright et al. 2000 [9], Wu, Qiu et al. 2005 [33], Lu, Weng et al. 2006 [25], Dong, Ramesh et al. 2010 [11], Salvati, Guandalini et al. 2017 [29].

High resolution satellite imagery, like Quickbird satellite imagery or even imagery from Landsat mission is also suitable in contrast with ground survey and Arial photo in terms of cost and time summarised by Alsalman, Abdullah Salman et al., 2011 [1]. Javed and Jocelyn, 2012 [18] also underlines the effectiveness of Google Earth satellite images for the classification of high, medium, and low population density and non-populated areas. Different other studies as Langford, Mitchel, 2013 [22], Checchi, Francesco, et al., 2013 [5], Bennie, Jonathan, et al., 2014 [3], Stevens, Forrest R., et al., 2015 [31], Lin, Changqing, et al., 2016 [23] are also depicting the usefulness of satellite images i.e. Quickbird, Landsat and MODIS in population estimation.

The cutting-edge infrastructure at FabSpace 2.0 Lab Darmstadt offers an incredible opportunity for answering complex social issues like population dynamics and supporting sustainable development policies, ideas and technologically -driven innovations with potential for markets using remote sensing and GIS tools. Therefore, the current task of ImageCLEF Remote 2017 is of great interest to explore the effectiveness of Sentinel-2 satellite imagery in such a complex operation.

2 Data

This study used Level-1C optical multispectral data from MSI (Multi Spectral Instrument) of Sentinel-2 mission. The data was pre-calibrated from the acquisition sensor [13], which is provided by Image CLEF Remote 2017 task [2]. This specific work used the 10 m resolution visible Red (Band 2 with 490 nm wavelength), Green (Band 3 with 560 nm wavelength) and Blue (Band 4 with 665 nm wavelength) and Near Infrared (Band 8 with 842 nm wavelength) bands [13]. These bands are used due to their high spatial resolution and large spectral wavelengths (from 490 nm to 842 nm) [13]. While the estimation of the population is based on the identification of households and built-up areas land covers. These four optical bands are used to build a false colour composite map, which is useful to make different land covers map [12]. The other demographic and geographic data was collected for the City of Lusaka of Zambia, and West Uganda from secondary sources and Image CLEF Remote 2017 task definition [2].

3 Data Processing

Data from Level-1C optical multispectral data from Sentinel-2 MSI (Multi Spectral Instrument) were pre-processed by Top of Atmospheric Correction to avoid dispute for the analysis [13]. The optical multispectral bands for City of Lusaka of Zambia, and West Uganda are pre-clipped according to the area extension for this study, which is defined by Mdecins Sans Frontires in 2016, where City of Lusaka of Zambia is divided into 73 areas of interest and West Uganda is divided into 17 areas of interest [17] [2].

4 Data Analysis

The satellite data provided by Image CLEF Remote 2017 task [2] and all others demographic and geographic information collected from secondary sources were analyzed to estimate population of selected region of Uganda and the city of Lusaka, Zambia [2]. The Sentinel-2 satellite imagery were analyzed by supervised and unsupervised classification using different methods and tools.

In the first set of run the provided bands 2,3,4 (VIS) and 8 (NIR) of Sentinel-2 images have been stacked [2]. Afterwards a supervised classification was carried out using the Semi-Automatic Classification Plug-in (SCP) in QGIS [7]. At first the regions of interest (ROI) or training input has been selected and separated as of different macro-classes like water surface, clouds, cloud shadow, streets, housing area, vegetation and agriculture. From this ROI the spectral signatures for defined classes are calculated considering the values of each pixel located in the same ROI. By applying Minimum Distance, Maximum Likelihood or Spectral Angle Mapping classification algorithm, each pixel is compared with the spectral signatures of the classes [7]. For this work, Minimum Distance and Maximum

Likelihood algorithm have been used. However, the Maximum Likelihood algorithm computes the probability distributions for the classes based on Bayes theorem [7].

The results have been reclassified to get raster data containing only housing areas. The reclassified raster data was vectorized to apply the polygon identity tool from SAGA [1] software. This tool used the provided shape data for Uganda and Zambia to add the respective city area codes to the created classification output. To merge the separate polygons of the identity tool results, the dissolve function in QGIS was used and the number of population of each polygon has been estimated. The areas of the dissolved classified polygons were calculated by the field calculator in QGIS. For the required population data in Lusaka, this area was multiplied by densities determined by dividing the population of Lusaka with the classified housing areas.

The second run of data analysis performed by K-Means Cluster Analysis [26] as unsupervised land classification and Maximum Likelihood Classification [7] as supervised land classification. K-Means Cluster Analysis was performed by Near Infrared band data for both study areas Lusaka and Uganda (Figure 1, 2 and Figure 3, 4). Maximum Likelihood Classification was performed by false colour composite map (Figure 5 and Figure 7) and by only the Near Infrared band for both study area (Figure 6 and Figure 8) [See the Annex-1].

Near Infrared band is appropriate for the good land classification and land cover change analysis in multi direction, primary focus on vegetation mapping [12], [14], [20], [10]. False color composite raster is also well suited to do the different land classifications. Here the false color composition is based on chronological sequences of Near Infrared band, Red band and Green bands whereby the blue band stays unused. Near infrared band is used primarily for vegetation land cover. Red band is used for mapping man-made objects, water, soil, and vegetation. Green band is used for mapping vegetation and deep water structures. Blue band is also used for atmosphere and deep water mapping [21], [4], [6]. Therefore, this study only highlighted the use of Red, Green, Blue, and Near Infrared bands as the study is focusing on the population estimation, which is depending on the classification of man-made built-up areas, vegetation or soil covers, and water bodies.

K-Means Cluster Analysis

K-Means Cluster Analysis as unsupervised land classification is based on 11 different clusters because within 11 clusters the lands are identical; however, this analysis was run by 5 clusters and 15 clusters separately, while 5 clusters showed less identical land covers and 15 clusters showed mixed land covers. The analysis is performed by SNAP (Sentinel Application Platform) version 5 provided by European Space Agency - ESA[2].

K-means is one of the simplest unsupervised learning algorithms that solve the well-known clustering problem [26]. The term "k-means" was first used by James MacQueen in 1967 [26]. The standard algorithm was first proposed by

[1] http://www.saga-gis.org/en/index.html
[2] http://step.esa.int/main/toolboxes/snap/

Stuart Lloyd in 1957 as a technique for pulse-code modulation, and published by Bell Labs in 1982 [24]. K-Means Cluster uses an iterative refinement technique it is called the k-means algorithm [24]. The K-means algorithm is an algorithm for putting N data points in an I-dimensional space into K clusters. Each cluster is parameterized by a vector m(k) called its mean. The data points will be denoted by x(n) where the superscript n runs from 1 to the number of data points N. Each vector x has I components xi. This will assume that the space that x lives in is a real space and that it has a metric that defines distances between points, for example,

$$d(x, y) = \frac{1}{2} \sum_{i}^{n} (X_i - Y_i)^2$$

Maximum Likelihood Classification

Maximum Likelihood Classification as supervised land classification is run with 4 different types of supervised land classes for City of Lusaka and 3 different types of supervised land classes for west Uganda (excluding Cloud), as

1. Built-Up areas (Including households, and manmade structures)
2. Vegetation (Including bare soils)
3. Waters (Including every existing water types)
4. Cloud

The supervised land classes are based on 75 identical training sites. The identification of training sites is based on ESRI base map[3], false colour composite map (Red, Green, Blue and Near Infrared band), and Near Infrared band.

The maximum likelihood classification works based on two principles

1. The cells in each class sample in the multidimensional space being normally distributed
2. Bayes' theorem of decision making

The tool considers both the variances and covariance of the class signatures when assigning each cell to one of the classes represented in the signature file. With the assumption that the distribution of a class sample is normal, a class can be characterized by the mean vector and the covariance matrix. Given these two characteristics for each cell value, the statistical probability is computed for each class to determine the membership of the cells to the class.

Maximum Likelihood algorithm calculates the probability distributions for the classes, related to Bayes theorem, estimating if a pixel belongs to a land cover class [7]. In particular, the probability distributions for the classes are assumed the form of multivariate normal models [28]. In order to use this algorithm, a sufficient number of pixels are required for each training area allowing for the calculation of the covariance matrix. The discriminate function, described by [28], is calculated for every pixel as:

[3] http://www.esri.com/data/basemaps

$$g_k(X) = lnp(C_k) - \frac{1}{2}ln|\sum_k| - \frac{1}{2}(X - Y_k)^t \sum_k^{-1}(X - Y_k)$$

Where:
C_k = land cover class k;
X = spectral signature vector of an image pixel;
p $(C_k) = probabilitythatthecorrectclassis C_k$;
$|\sum_k| = determinantofthecovariancematrixofthedatainclass C_k$;
$\sum_k^{-1} = inverseofthecovariancematrix$;
Y_k = spectral signature vector of class k.

4.1 Results

The summary of the modeled output is presented in the table 1, where the measured data was validated with the ground truth provided by Image CLEF remote 2017 [2]. The result from final run (non-official run) showing statistics for population for Uganda (UGD) and City of Lusaka, Zambia (ZMB) has sum of deltas of 19 and 34, RMSE of 2199 and 15505 and Pearson correlation of 0.87 and 0.81 respectively. The statistics for the number of dwellings/household for UGD and ZMB are sum of deltas of 24 and 34, RMSE of 638 and 3073 and Pearson correlation of 0.87 and 0.81 respectively. In the case of Lusaka the best result was calculated using the supervised Maximum Likelihood Classification method where using only near infrared band showed better result than the false color composite raster (i.e. R,G,B and NIR stack image). While for Uganda the best results were obtained by K-means unsupervised clustering using near infrared band as an input and the best result was obtained in the first run thereby parameters remains same in the final run.

Lusaka District, Zambia

In the case of City of Lusaka, Zambia, from the literature search the total district area is 360 Km^2, the total population is 2,330,200 as of the population projection on 01.07.2016, the average household size is 4.9 person per household and the density is 6,472 person/Km^2 with the change rate of +5.17 percent per year (2010 to 2016) where the urban population is 40.2 percent of overall population [27]. In the Image CLEF remote 2017 challenge [2], the whole Lusaka city was divided in 73 geographical units and population was estimated and validated with ground truth for each geographical unit.

According to the K-Means Cluster Analysis it is found that the total district built-up area including mixed use area is 318.59 Km^2 and the total population is 1,542,496 and total household 314,795.

From Maximum Likelihood Classification for the City of Lusaka as of the area denoted by the task with false color composite raster (R, G, B and NIR), it is found that the district built-up area is 145.95 Km^2 the total population is 1,324,568 and total household is 270,320. The result from the classification using

Table 1. Details of the classifications results (German FabSpace) [2]

Population			
Study Area	**Sum**	**Delta**	**RMSE Pearson**
1st Run			
Uganda	19	2,199	0.87
Zambia	68	30,510	0.11
Final Run			
Uganda	19	2,199	0.87
Zambia	34	15,505	0.81

House Count			
Study Area	**Sum**	**Delta**	**RMSE Pearson**
1st Run			
Uganda	24	638	0.87
Zambia	76	6,055	0.11
Final Run			
Uganda	24	638	0.87
Zambia	34	3,073	0.81

only near infrared band shows the built-up area is 174.48 Km^2, the total population is 1,540,516 and the number of household is 314,390. In the calculation of population, first the overall population was estimated and then 40.2 percent of urban population was added to reach the highest accuracy.

West Uganda

The current population of Uganda is 41,473,759 as of May, 2017, based on the latest United Nations estimation, the population density in Uganda is 209 per Km^2 and 5 persons per household, the total land area is 199,816 Km^2, and 17.3 percent of the population is counted as urban population [27]. According to the challenge description [2] the 17 geographical unit was selected to estimate population and validated afterwards with the ground truth.

According to the K-Means Cluster Analysis it is found that the total district built-up area is 38.80 Km^2 and the total population is 40,291 and the total number of households are 8,058.

The Maximum Likelihood Classification using only NIR band results shows the number of population for the selected 17 regions are 43,963 including 17 percent urban population on top of the total population and the total household estimated as 8,792 where the calculated built-up area is 23.03 Km^2. While, using RGB and NIR stack data shows the total population is 54,043, total households are 10,808 and the total area is 22.20 Km^2.

5 Conclusion

The calculation of population by satellite data is based on the estimation of household areas and built up areas and the population density. The identifi-

cation of land classification for household and built-up areas is not uniform, it depends on the area type, and it is challenging due to the heterogeneous spectral reflectance from mixed up different household and built up areas with other land use types as bare soil or dense green vegetation. The problem is more severe in the case of differentiating reflectance value of building rooftop, road and bare soil as all has almost same type of materials. Beside these limitations, the number of floors of any buildings is not measured for this activity, because this pilot task used Sentinel-2 MSI sensor data which is not sufficient to perform this. However, the height of buildings or any structure could be measured by the objects shadow detection analysis, but it is time consuming and will be challenging to achieve the necessary analytical accuracy. Though, there is an emerging opportunity to make the study more effective. Although, this pilot task used both unsupervised and supervised land classifications to minimize the calculation error as much as possible. The supervised land classifications are done by Maximum Likelihood Classification algorithm and unsupervised land classification through K-means cluster analysis with more than 80 percent accuracy. This particular pilot task found the fusion of unsupervised and supervised land classifications for household and built up areas with Sentinel-2 MSI sensor is promising to calculate the population.

However, there were some difficulties to run the classification as for the city of Lusaka, big challenges were to segregate agricultural areas that have been classified as housing area and the big gaps of density between poor and wealthy housing areas. In Uganda it was also difficult to mark off the built-up areas from the areas with bushland and open vegetation. For Uganda, the classification faced problems to detect the distinct housing areas and differentiate these with other macro-classes due to same spectral signatures. Moreover, the area in Uganda is rural with only few settlements and low population density. While in Lusaka the difficulties are the differentiation of housing areas from informal settlements with high population density to high income areas.

6 Acknowledgement

This work is a part of the FabSpace 2.0[4] project that received funding from the European Unions Horizon 2020 Research and Innovation programme under the Grant Agreement n693210.

References

1. Abdullah Salman Alsalman and Abdullah Elsadig Ali. Population estimation from high resolution satellite imagery: A case study from khartoum. *Emirates Journal for Engineering Research*, 16(1):63–69, 2011.
2. Helbert Arenas, Bayzidul Islam, and Josiane Mothe. Overview of the ImageCLEF 2017 Population Estimation Task. In *CLEF 2017 Labs Working Notes*, CEUR

[4] https://www.fabspace.eu/

Workshop Proceedings, Dublin, Ireland, September 11-14 2017. CEUR-WS.org <http://ceur-ws.org>.

3. Jonathan Bennie, Thomas W Davies, James P Duffy, Richard Inger, and Kevin J Gaston. Contrasting trends in light pollution across europe based on satellite observed night time lights. *Scientific reports*, 4:3789, 2014.
4. Larry Biehl and David Landgrebe. Multispeca tool for multispectral–hyperspectral image data analysis. *Computers & Geosciences*, 28(10):1153–1159, 2002.
5. Francesco Checchi, Barclay T Stewart, Jennifer J Palmer, and Chris Grundy. Validity and feasibility of a satellite imagery-based method for rapid estimation of displaced populations. *International journal of health geographics*, 12(1):4, 2013.
6. Valerie C Coffey. Multispectral imaging moves into the mainstream. *Optics and Photonics News*, 23(4):18–24, 2012.
7. Luca Congedo. Semi-automatic classification plugin documentation. *Release*, 4(0.1):29, 2016.
8. Thomas Dietz and Eugene A Rosa. Rethinking the environmental impacts of population, affluence and technology. *Human ecology review*, 1(2):277–300, 1994.
9. Jerome E Dobson, Edward A Bright, Phillip R Coleman, Richard C Durfee, and Brian A Worley. Landscan: a global population database for estimating populations at risk. *Photogrammetric engineering and remote sensing*, 66(7):849–857, 2000.
10. Jinwei Dong, Xiangming Xiao, Michael A Menarguez, Geli Zhang, Yuanwei Qin, David Thau, Chandrashekhar Biradar, and Berrien Moore. Mapping paddy rice planting area in northeastern asia with landsat 8 images, phenology-based algorithm and google earth engine. *Remote sensing of environment*, 185:142–154, 2016.
11. Pinliang Dong, Sathya Ramesh, and Anjeev Nepali. Evaluation of small-area population estimation using lidar, landsat tm and parcel data. *International Journal of Remote Sensing*, 31(21):5571–5586, 2010.
12. John R Dymond, Agnes Begue, and Danny Loseen. Monitoring land at regional and national scales and the role of remote sensing. *International Journal of Applied Earth Observation and Geoinformation*, 3(2):162–175, 2001.
13. European Space Agency ESA. Suhet: Sentinel-2 user handbook. esa standard document, 2015.
14. Matthew C Hansen, Peter V Potapov, Rebecca Moore, Matt Hancher, SA Turubanova, Alexandra Tyukavina, David Thau, SV Stehman, SJ Goetz, TR Loveland, et al. High-resolution global maps of 21st-century forest cover change. *science*, 342(6160):850–853, 2013.
15. John P Holdren and Paul R Ehrlich. Human population and the global environment: Population growth, rising per capita material consumption, and disruptive technologies have made civilization a global ecological force. *American scientist*, 62(3):282–292, 1974.
16. Lori M Hunter. *The environmental implications of population dynamics*. Rand Corporation, 2000.
17. Bogdan Ionescu, Henning Müller, Mauricio Villegas, Helbert Arenas, Giulia Boato, Duc-Tien Dang-Nguyen, Yashin Dicente Cid, Carsten Eickhoff, Alba Garcia Seco de Herrera, Cathal Gurrin, Bayzidul Islam, Vassili Kovalev, Vitali Liauchuk, Josiane Mothe, Luca Piras, Michael Riegler, and Immanuel Schwall. Overview of ImageCLEF 2017: Information extraction from images. In *Experimental IR Meets Multilinguality, Multimodality, and Interaction 8th International Conference of the CLEF Association, CLEF 2017*, volume 10456 of *Lecture Notes in Computer Science*, Dublin, Ireland, September 11-14 2017. Springer.

18. Yousra Javed, Muhammad Murtaza Khan, and Jocelyn Chanussot. Population density estimation using textons. In *Geoscience and Remote Sensing Symposium (IGARSS), 2012 IEEE International*, pages 2206–2209. IEEE, 2012.
19. John R Jensen and Dave C Cowen. Remote sensing of urban/suburban infrastructure and socio-economic attributes. *Photogrammetric engineering and remote sensing*, 65:611–622, 1999.
20. Kasper Johansen, Stuart Phinn, and Martin Taylor. Mapping woody vegetation clearing in queensland, australia from landsat imagery using the google earth engine. *Remote Sensing Applications: Society and Environment*, 1:36–49, 2015.
21. David A Landgrebe. The development of a spectral-spatial classifier for earth observational data. *Pattern Recognition*, 12(3):165–175, 1980.
22. Mitchel Langford. An evaluation of small area population estimation techniques using open access ancillary data. *Geographical Analysis*, 45(3):324–344, 2013.
23. Changqing Lin, Ying Li, Alexis KH Lau, Xuejiao Deng, KT Tim, Jimmy CH Fung, Chengcai Li, Zhiyuan Li, Xingcheng Lu, Xuguo Zhang, et al. Estimation of long-term population exposure to pm 2.5 for dense urban areas using 1-km modis data. *Remote sensing of environment*, 179:13–22, 2016.
24. Stuart Lloyd. Least squares quantization in pcm. *IEEE transactions on information theory*, 28(2):129–137, 1982.
25. Dengsheng Lu, Qihao Weng, and Guiying Li. Residential population estimation using a remote sensing derived impervious surface approach. *International Journal of Remote Sensing*, 27(16):3553–3570, 2006.
26. James MacQueen et al. Some methods for classification and analysis of multivariate observations. In *Proceedings of the fifth Berkeley symposium on mathematical statistics and probability*, volume 1, pages 281–297. Oakland, CA, USA., 1967.
27. Alex B Makulilo. The context of data privacy in africa. In *African Data Privacy Laws*, pages 3–23. Springer, 2016.
28. John A Richards. *Remote sensing digital image analysis: an introduction*. Springer Science & Business Media, 2012.
29. Luca Salvati, Alessio Guandalini, Margherita Carlucci, and Francesco Maria Chelli. An empirical assessment of human development through remote sensing: Evidences from italy. *Ecological Indicators*, 78:167–172, 2017.
30. Uwe A Schneider, Petr Havlík, Erwin Schmid, Hugo Valin, Aline Mosnier, Michael Obersteiner, Hannes Böttcher, Rastislav Skalskỳ, Juraj Balkovič, Timm Sauer, et al. Impacts of population growth, economic development, and technical change on global food production and consumption. *Agricultural Systems*, 104(2):204–215, 2011.
31. Forrest R Stevens, Andrea E Gaughan, Catherine Linard, and Andrew J Tatem. Disaggregating census data for population mapping using random forests with remotely-sensed and ancillary data. *PloS one*, 10(2):e0107042, 2015.
32. David N Weil, Oded Galor, et al. Population, technology, and growth: From malthusian stagnation to the demographic transition and beyond. *American Economic Review*, 90(4):806–828, 2000.
33. Shuo-sheng Wu, Xiaomin Qiu, and Le Wang. Population estimation methods in gis and remote sensing: a review. *GIScience & Remote Sensing*, 42(1):80–96, 2005.

ANNEX-1: Classification results from the final run.

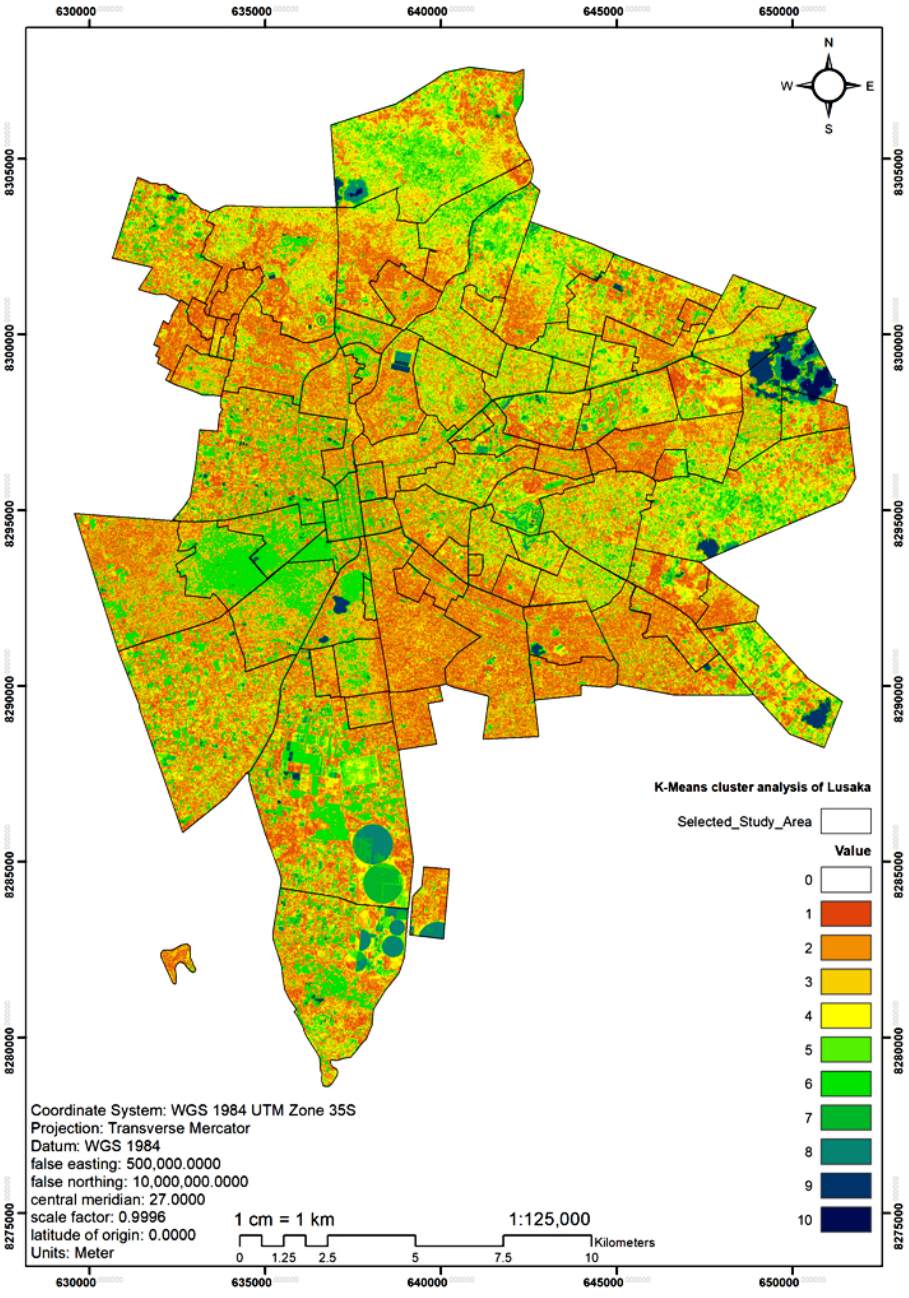

Fig. 1. K-Means Cluster Analysis of City of Lusaka (Source: FabSpace 2.0 Darmstadt lab, 2017).

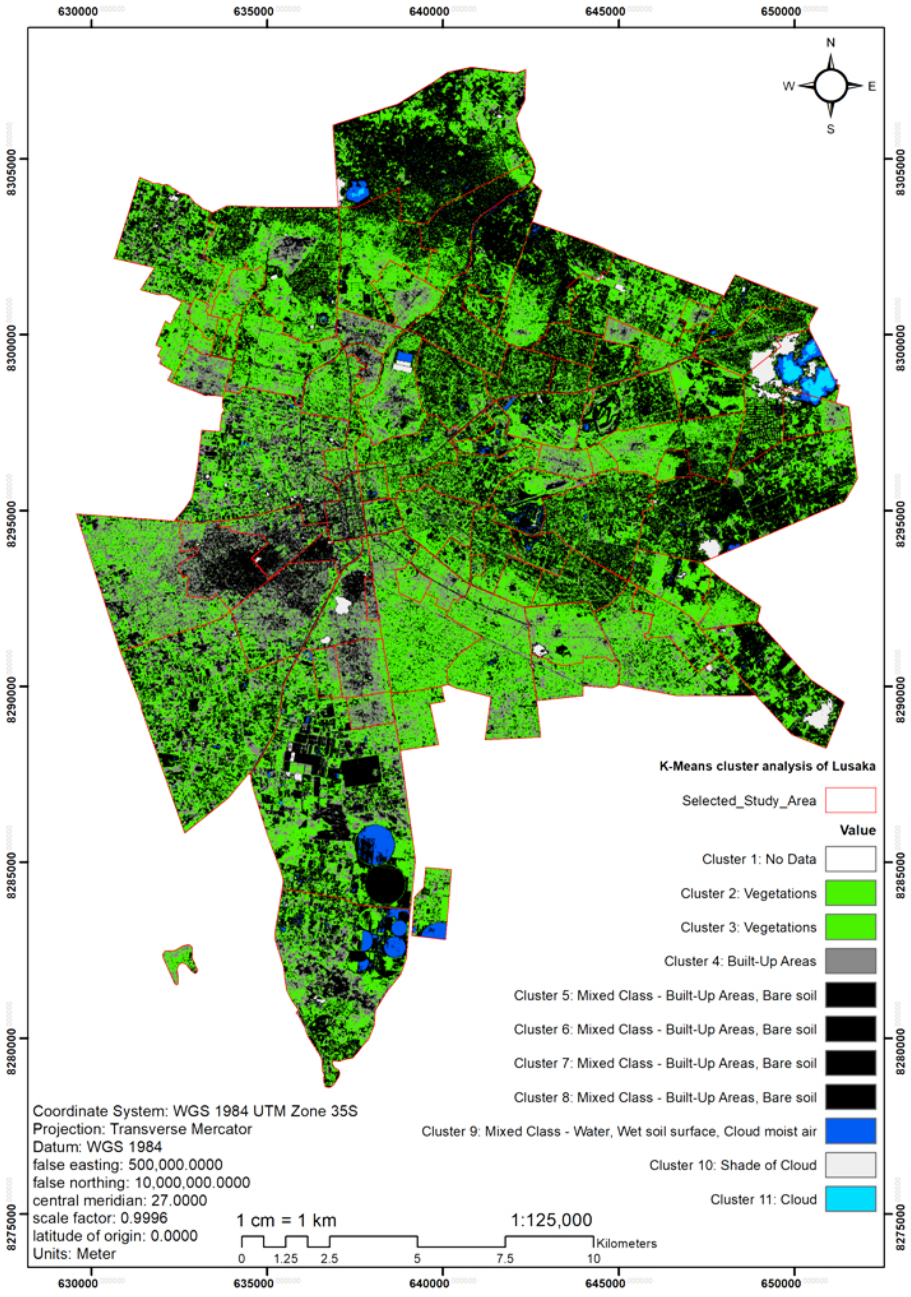

Fig. 2. K-Means Cluster Analysis of City of Lusaka supervised by Maximum Likelihood classification (Source: FabSpace 2.0 Darmstadt lab, 2017).

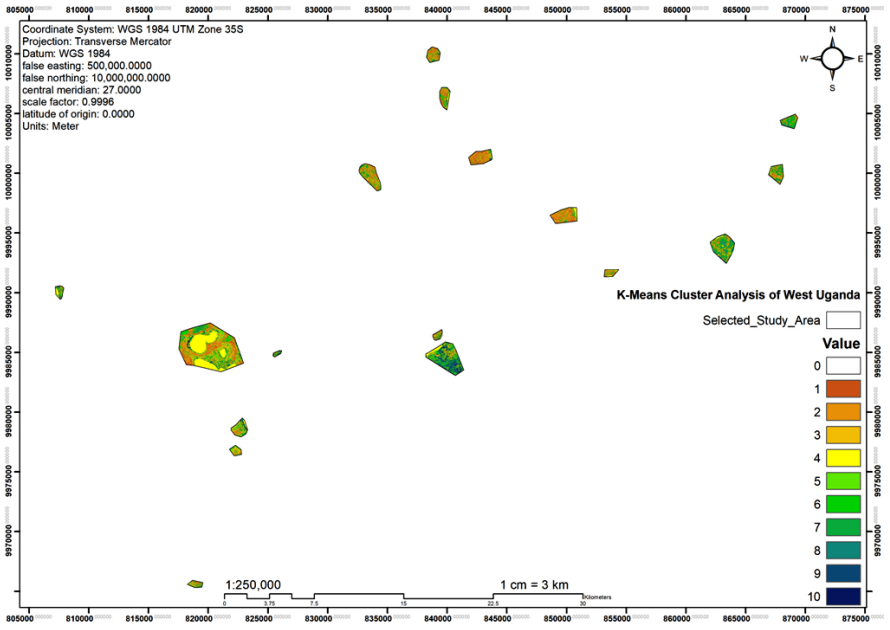

Fig. 3. K-Means Cluster Analysis of West Uganda (Source: FabSpace 2.0 Darmstadt lab, 2017).

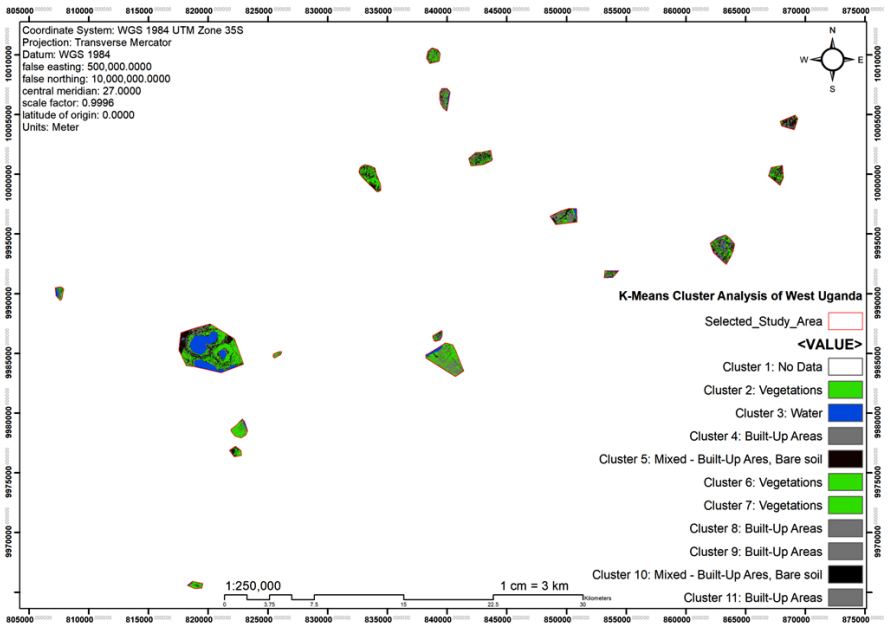

Fig. 4. K-Means Cluster Analysis of West Uganda supervised by Maximum Likelihood classification (Source: FabSpace 2.0 Darmstadt lab, 2017).

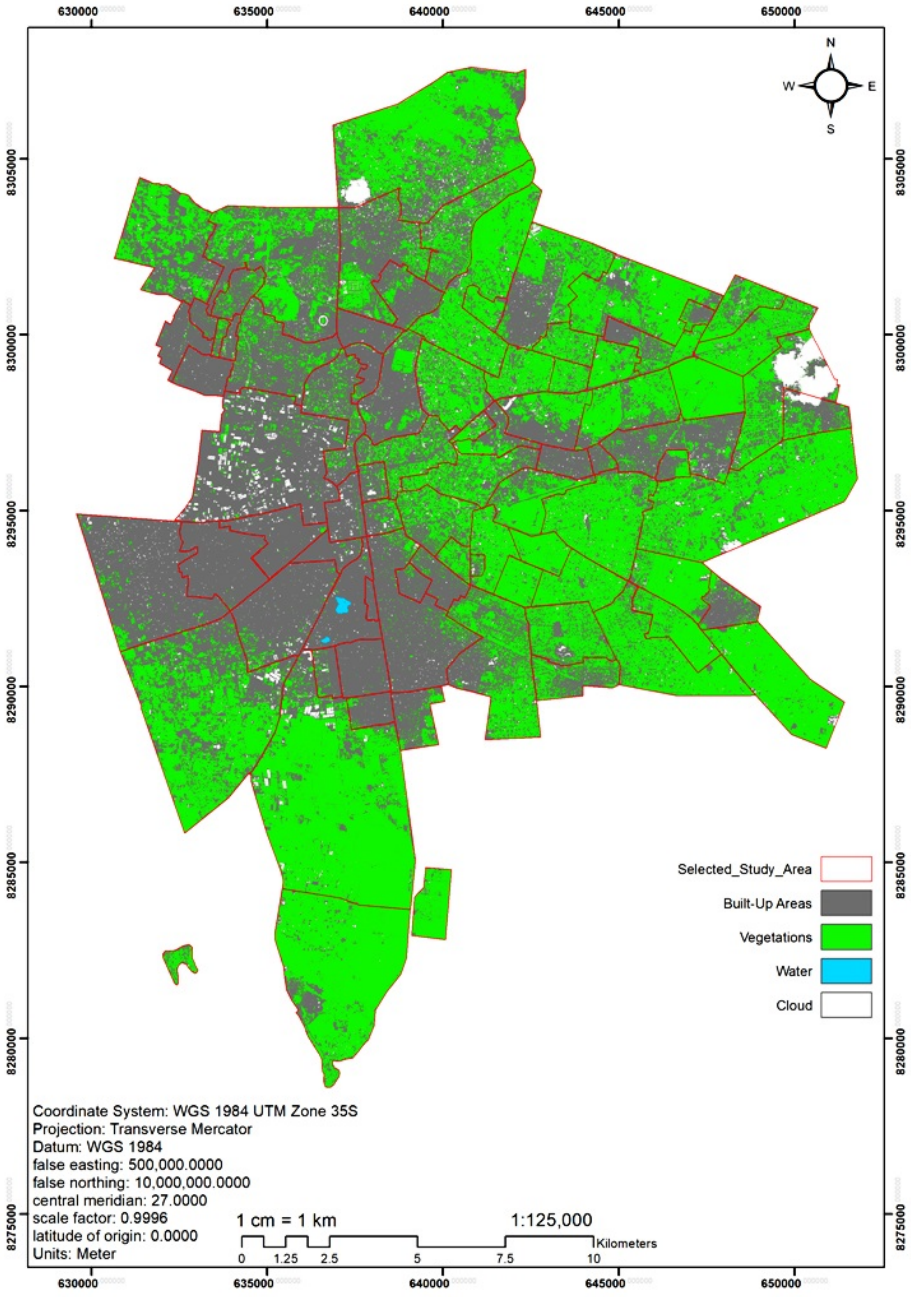

Fig. 5. Maximum Likelihood Classification of City of Lusaka with False colour composite raster (Source: FabSpace 2.0 Darmstadt lab, 2017).

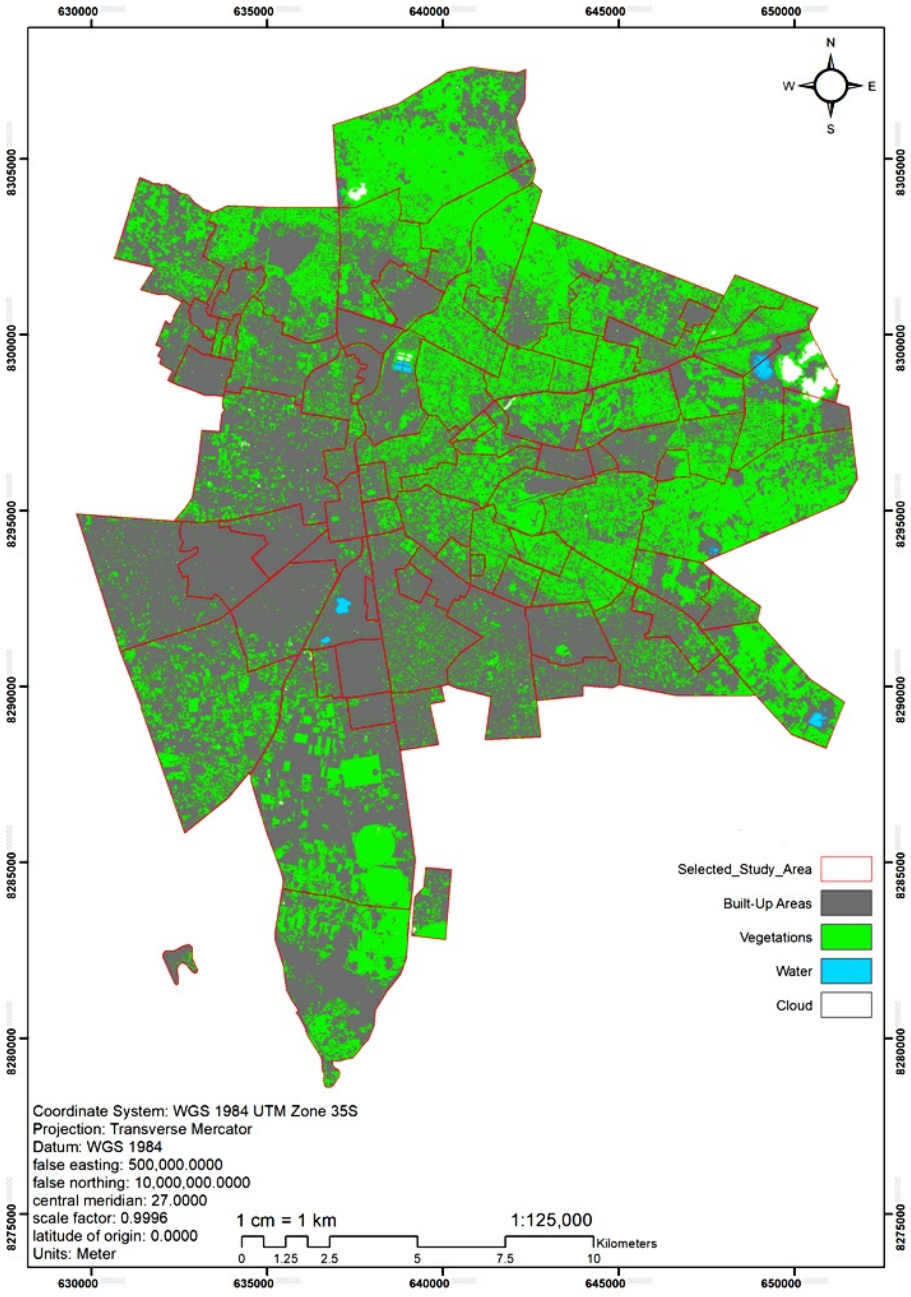

Fig. 6. Maximum Likelihood Classification of City of Lusaka with Near Infrared band (Source: FabSpace 2.0 Darmstadt lab, 2017).

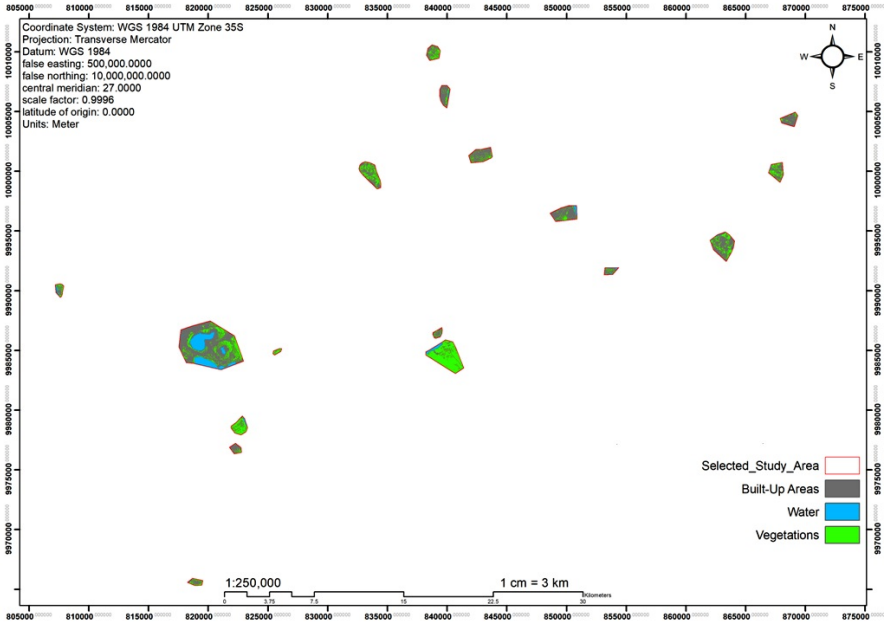

Fig. 7. Maximum Likelihood Classification of West Uganda with False colour composite raster (Source: FabSpace 2.0 Darmstadt lab, 2017).

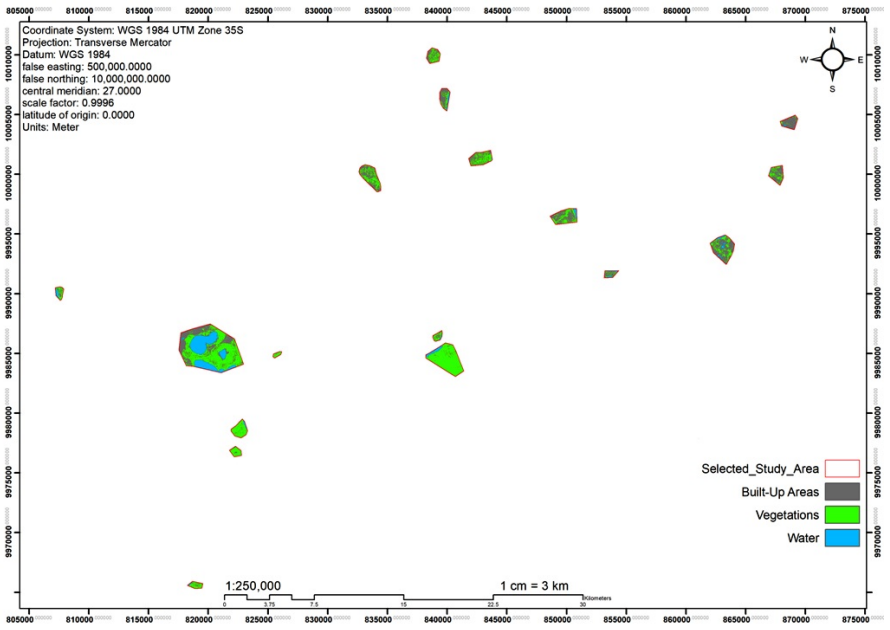

Fig. 8. Maximum Likelihood Classification of West Uganda with Near Infrared band (Source: FabSpace 2.0 Darmstadt lab, 2017).